Catalysis Science & Technology

ROYAL SOCIETY OF CHEMISTRY

PAPER

View Article Online
View Journal

Check for updates

Cite this: DOI: 10.1039/d0cy01526a

Room temperature and atmospheric pressure aqueous partial oxidation of ethane to oxygenates over AuPd catalysts†

Yu Lei Wang, ‡ Sadi Gurses, ‡ Noah Felvey and Coleman X. Kronawitter *

Received 9th June 2020,
Accepted 14th August 2020

DOI: 10.1039/d0cy01526a

rsc.li/catalysis

New modes of chemical manufacturing based on small-scale, distributed facilities have been proposed to supplement many existing production operations in the chemical industry, including the synthesis of value-added products from light alkanes. Motivated by this prospect, herein the aqueous partial oxidation of ethane over unsupported AuPd nanoparticle catalysts is investigated, with emphasis on outcomes for reactions occurring at 21 °C and 1 bar ethane. When H_2O_2 is used as an oxidant, the system generates numerous C_2 oxygenates, including ethyl hydroperoxide/ethanol, acetaldehyde, and acetic acid. Ethyl hydroperoxide is found to be the primary product resulting from the direct oxidation of ethane: it is produced with 100% selectivity in batch reactions with short durations and with low initial H_2O_2 concentrations. At longer times or in more oxidizing conditions, deeper product oxidations expectedly occur. In batch experiments, the maximum observed yield of oxygenates is 7707 μmol g_{AuPd}^{-1} h^{-1}. Product distributions differ when H_2O_2 is replaced by H_2 and O_2 in the headspace. Additionally, to simulate a scenario wherein H_2O_2 is produced on-site and to study ethane oxidation in steady, low H_2O_2 concentrations over 50 h, a semi-batch configuration facilitating continuous injection of dilute H_2O_2 was implemented. These efforts showed that H_2O_2 can serve as an oxygenate-selective oxidant of ethane when its concentration is kept low during reaction. These and other experimental results, as well as initial computational results using density functional theory, suggest that paths forward for aqueous ethane conversion exist, and systems should be engineered to emphasize product stabilization.

Introduction

The rapid discovery of geographically dispersed sources of unconventional feedstocks has provided considerable motivation for the chemical industry to pursue distributed chemical manufacturing as a supplemental mode of production.[1,2] Advances in renewable energy technologies and the associated reduction in energy costs at remote locations provide further impetus for development of a distributed network of chemical production facilities. Given the reduced scale and the nature of geographically distributed resources, new technologies that facilitate the catalytic direct functionalization of small molecules in mild conditions (low temperature and pressure and with minimal environmental impact) are expected to be paramount for any significant adoption of distributed chemical manufacturing schemes.

The widespread use of small molecule feedstocks would have parallel disruptive effects on the global chemical industry, which currently relies heavily on conventional petroleum resources. Molecules of interest in this context include the light alkanes – the primary constituents of natural gas – whose global abundance and utility have been made apparent by the recent shale gas revolution,[3,4] as well as CO_2, H_2O, O_2, and N_2, the utilization of which is considered critical for future sustainability in the energy sector as well as other high-energy-use sectors, including chemical synthesis.[5–8]

In order to develop these technologies, it is essential to explore the behaviors of catalytic systems in relevant mild conditions – especially near room temperature and atmospheric pressure. Although the optimal operating conditions for catalysis will vary greatly among relevant reactions and processes, even for systems that are required to operate at elevated temperatures, knowledge of the reactivity and stability of products in the reaction medium at room temperature is of critical value.

Oxidative functionalization of light alkanes is particularly relevant in this context. The local generation of products that exist in the liquid phase at standard temperature and

Department of Chemical Engineering, University of California, Davis, CA 95616, USA. E-mail: ckrona@ucdavis.edu

† Electronic supplementary information (ESI) available. See DOI: 10.1039/d0cy01526a

‡ These authors contributed equally to this work.

pressure would alleviate distribution and utilization constraints that result from the transportation of large volumes of flammable gases from remote sources.[9] Although the aliphatic C–H bonds of light alkanes are strong, a number of catalysts have been studied for the low-temperature oxidative functionalization of alkanes to produce oxygenates including alcohols, aldehydes, and acids.[10–12] Ethane is typically the second-most abundant constituent of natural gas, and although its direct low-temperature partial oxidation has not received the same level of attention as that of methane,[13] it is a promising feedstock for the distributed production of oxygenates in mild conditions.[9] Here, the direct partial oxidation of ethane at unsupported colloidal AuPd nanoparticle catalysts suspended in water is examined.

Results and discussion

Stabilizer-free AuPd (1 : 1 molar ratio) nanoparticles were prepared *via* adaptation of standard colloidal synthesis procedures involving reduction of metal precursors ($PdCl_2$ and $HAuCl_4$), followed by heat treatment (100 °C). Complete synthesis details are provided in the Experimental methods section of the ESI.† An X-ray diffractogram (XRD) of the AuPd catalyst particles (Fig. 1a) indicates a diffraction pattern with peaks centered at intermediate values between those of metallic Au (PDF#04-0784) and metallic Pd (PDF#46-1043), confirming the formation of an alloy.[14] High-angle annular dark-field scanning transmission electron microscopy (HAADF-STEM) images reveal that the AuPd crystals possess multiply twinned lattice fringes, but nanoparticle agglomeration resulting from dispersion onto the TEM grid prevents distinguishing the prevalence of icosahedral *versus* cuboctahedral structure, which has been true for other studies (Fig. 1b and c).[15,16] The AuPd nanoparticles have a mean diameter of 4.93 nm with a narrow particle-size distribution (Fig. 1d). Au 4f and Pd 3d X-ray photoelectron spectroscopy (XPS) results show that heat treatment of AuPd results in the formation of oxidized species Pd^{2+} and Au^{3+} (Fig. 1e and f), as has been observed previously in AuPd-based catalysts.[17] However, no distinct surface phases were detected by XRD or energy dispersive X-ray spectroscopy (EDX) mapping (Fig. S1†), a typical phenomenon reported in literature.[18] Three independent measurements were taken to determine the compositions of the catalysts: XPS, inductively coupled plasma atomic emission spectroscopy (ICP-AES) and EDX analysis (Table S1†). The Au : Pd molar ratio was determined by all techniques to be nearly 1 : 1.

Catalytic activity was tested in a purpose-built reactor with all wetted components manufactured from chemically resistant PEEK plastic. In a typical batch experiment, 5 mL aqueous AuPd colloid (6.6 μmol of metals) was combined with hydrogen peroxide (H_2O_2) at room temperature (21 °C)

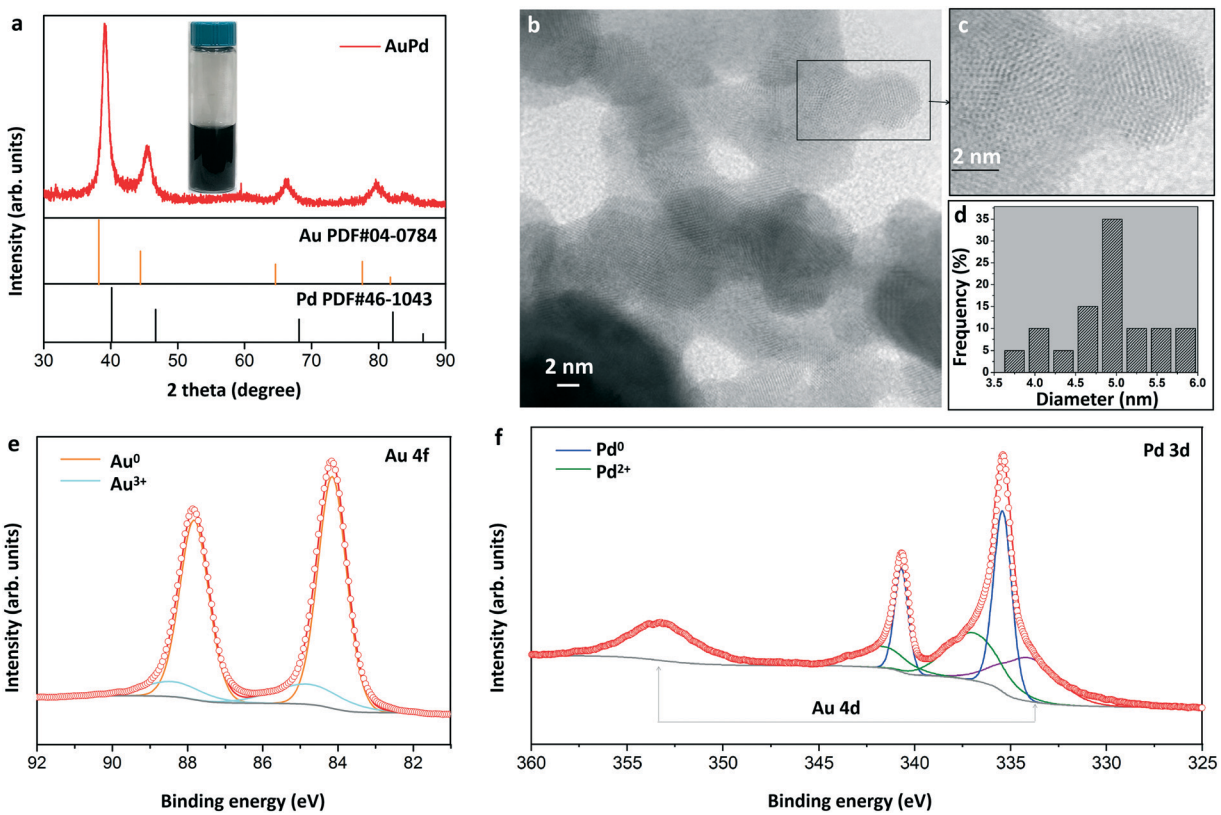

Fig. 1 (a) XRD pattern of the nanoparticulate AuPd catalysts. Inset: A photograph of the aqueous AuPd colloidal suspension. (b) STEM image of AuPd catalysts. (c) Magnification of individual AuPd nanoparticles. (d) Size distribution of AuPd nanoparticles. (e and f) XPS spectra of AuPd in Au 4f and Pd 3d regions.

with 1 bar (1 atm) of ethane (C_2H_6). To our best knowledge, this work represents the first example for aqueous partial oxidation of ethane to oxygenates occurring at room temperature and atmospheric pressure (Table S2†). Liquid-phase products were quantified using ^{1}H NMR through independent calibration curves generated from chemical standards (Fig. S2†), and gas-phase products were analyzed by gas chromatography (GC).

Fig. 2 provides results of several aqueous batch reactor studies. The data indicate that AuPd catalyzes the partial oxidation of ethane to various oxygenates at room temperature and atmospheric pressure in the presence of H_2O_2. To confirm this result, several control experiments were performed. It was determined that no liquid oxygenates were observed in the absence of either C_2H_6 or H_2O_2, indicating that H_2O_2 was necessary to initiate the C_2H_6 oxidation reaction, similar to observations made in other reports.[10] Additionally, the potential influence of dissolved metal ions (with equivalent 6.6 μmole dissolved metal) was investigated; no products were observed in the presence of Au and Pd ions but in the absence of AuPd (Table S3,† entry 1). In all C_2H_6 oxidation experiments, analysis of the headspace by GC revealed no CO_2 was present; however the relatively high solubility of CO_2 in water[19] prevents a definitive claim that no complete oxidation occurs (see discussion later in this report for evidence of acetic acid oxidation to CO_2 in alternate conditions used for mechanistic studies).

Fig. 2a provides the quantities of oxygenates produced and of H_2O_2 consumed at seven different initial H_2O_2 concentrations ($[H_2O_2]_{initial}$). It is shown that $[H_2O_2]_{initial}$ influences the product yields and selectivities, as well as the efficiency of H_2O_2 utilization in the oxidative C-H functionalization process. The selectivity to ethyl hydroperoxide (CH_3CH_2OOH, EtOOH) was 100% when the $[H_2O_2]_{initial}$ was lower than 30 mM. Given this remarkable result, the batch reaction with 10 mM $[H_2O_2]_{initial}$ was repeated seven times to verify that EtOOH was the sole product in these conditions. At higher $[H_2O_2]_{initial}$, acetaldehyde (CH_3CHO) and acetic acid (CH_3COOH) were observed (Fig. 2a). Additionally, it was observed that the maximum amount of liquid oxygenates (7707 μmol g_{AuPd}^{-1} h^{-1}) was obtained for 200 mM $[H_2O_2]_{initial}$ (Fig. 2a and S3†). The efficiency of H_2O_2 utilization was also quantified. The gain factor (defined as mol oxygenates/mol H_2O_2 consumed)[10] was highest for low-$[H_2O_2]_{initial}$ reactions (Table S4,† entries 1–7). This phenomenon has been previously observed[10] and can be attributed to the fact that H_2O_2 adsorption and decomposition competes with C_2H_6 adsorption for surface sites.[19,20] When the reaction whose results are reported in Fig. 2c was studied with 10 bar C_2H_6 and the same $[H_2O_2]_{initial}$, a much greater quantity of EtOOH was formed (Fig. S4†), which is consistent with the existence of a competition for reactant adsorption.

In the reactions above, the decomposition products of H_2O_2 (ref. 21) are the active oxidants of the dissolved alkanes;

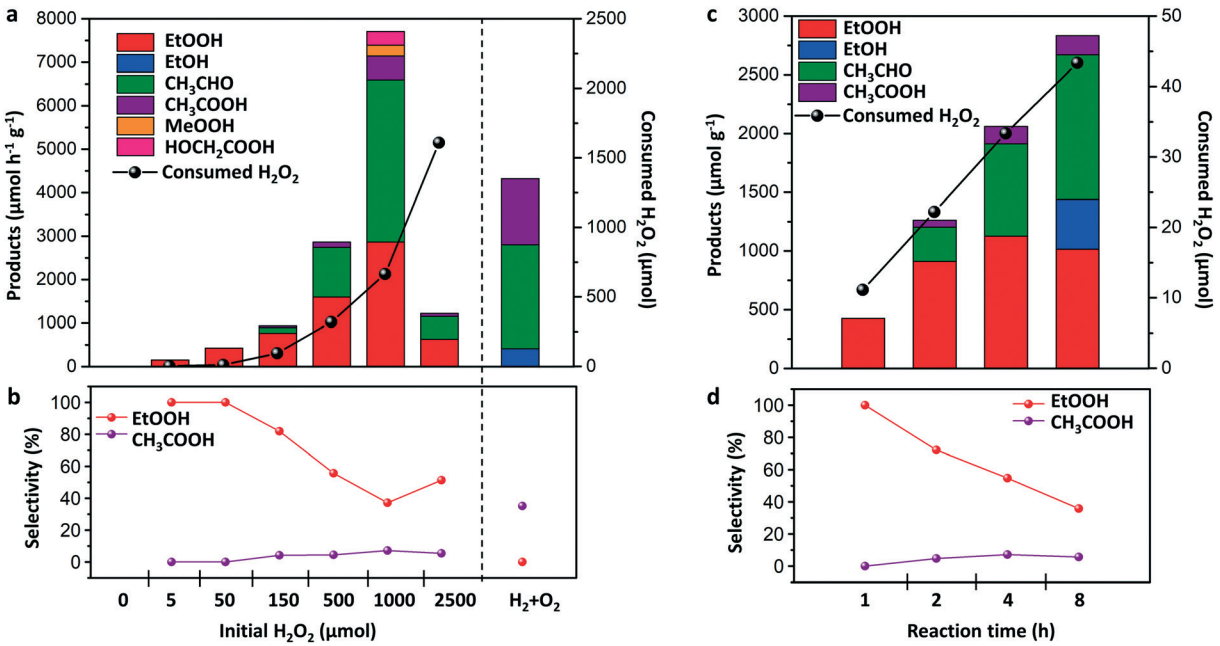

Fig. 2 Catalytic activity of unsupported AuPd nanoparticles for C_2H_6 oxidation. (a) Quantities of oxygenates produced and of H_2O_2 consumed for seven initial quantities of H_2O_2, corresponding to 0, 1, 10, 30, 100, 200, and 500 mM $[H_2O_2]_{initial}$, respectively. The right-hand side shows results generated in the absence of H_2O_2 but in the presence of a H_2/O_2 mixture. Reaction conditions: 5 mL; 1 mg AuPd; 21 °C; 1 h; 1000 rpm; 1 bar C_2H_6 or 2.4 bar gas mixture (4.17% H_2, 16.7% O_2, 37.5% N_2 and 41.6% C_2H_6). (b) Selectivities of EtOOH and CH_3COOH for reactions in (a). (c) Quantities of oxygenates produced and of H_2O_2 consumed for multiple reaction times. Reaction conditions: 5 mL; 1 mg AuPd; 10 mM $[H_2O_2]_{initial}$ (50 μmol); 1 bar C_2H_6; 21 °C; 1–8 h; 1000 rpm. (d) Selectivities to EtOOH and CH_3COOH for reactions in (c).

the results above suggest the existence of competition and cooperativity between C_2H_6 oxidation and H_2O_2 decomposition. H_2O_2 is itself a valuable commodity chemical – it is desirable to generate this compound or its reactive fragments *in situ* from O_2 and H_2. To explore the efficacy of this approach to the partial oxidation of ethane at unsupported AuPd nanoparticles, ethane was co-fed with O_2 and H_2 to the reactor in the absence of H_2O_2. The righthand sides of Fig. 2a and b show the results of these experiments. It was observed that the distribution of products differs considerably from that obtained through external H_2O_2. Specifically, a much higher ratio of CH_3COOH to EtOOH was obtained through co-fed H_2 and O_2. It was also observed that ethanol (CH_3CH_2OH, EtOH) comprised a significant fraction of products, which was not observed through direct oxidation by H_2O_2.

Direct comparison of C_2H_6 oxidation rate resulting from *in situ* reaction of H_2 and O_2 and from a finite $[H_2O_2]_{initial}$ is difficult because the instantaneous concentration of H_2O_2 and its reactive fragments cannot be known. However, a reasonable approximation is possible by recognizing that in the catalytic synthesis of H_2O_2 at AuPd ($H_2 + O_2 \rightarrow H_2O_2$) in these conditions H_2 is the limiting reactant, which has been established in prior literature.[22,23] If all H_2 were consumed and converted transiently to H_2O_2, the initial partial pressure of H_2 in the experiment corresponds to 87 μmol H_2O_2 (17.4 mM) generated over the course of the batch reaction. The total quantity of oxygenates generated through reaction of co-fed H_2 and O_2 (*ca.* 4320 μmol h^{-1} g_{cat}^{-1}) was 5–10 times greater than that was observed from reaction with H_2O_2 (425 and 934 μmol h^{-1} g_{cat}^{-1} for 10 and 30 mM $[H_2O_2]_{initial}$). It was considered that the presence of additional O_2 in the *in situ* experiments could influence product yields, but it was determined that this could be neglected: O_2 was also present in all experiments involving finite $[H_2O_2]_{initial}$ because it is a primary H_2O_2 decomposition product, and was quantified (Table S4†).

Based on these observations, the most reasonable initial interpretation is that the positive effects on oxygenate yield and the change in product distributions resulting from co-fed H_2 and O_2 originate from the presence of molecular H_2. Park *et al.* reported that molecular H_2 can be easily dissociated into atomic hydrogen (H*) over Pd atoms.[24] The H* could combine with molecular O_2 to produce H_2O_2. Most likely, intermediates generated during this process activate C_2H_6 and promote C_2H_6 oxidation. The observed EtOH could originate from direct C_2H_6 oxidation but also from EtOOH reduction by H*; this initial report of this catalysis does not facilitate direct determination of the mechanistic origin of EtOH in reactions with co-fed H_2 and O_2. Further dedicated mechanistic studies are underway to understand the distinguishing characteristics of catalysis driven by co-fed H_2 and O_2.

The 100% selectivity toward EtOOH observed at low $[H_2O_2]_{initial}$ (Fig. 2a and b) motivated further time-online experiments of the reaction with fixed $[H_2O_2]_{initial}$ (10 mM) (Fig. 2c and d). Both the total amount of liquid oxygenates and gain factor correlated positively with reaction time (Table S4,† entries 3, 8–10). With increasing reaction time, CH_3CHO and CH_3COOH were observed (Fig. 2c), consistent with sequential oxidation of EtOOH to CH_3CHO and then CH_3COOH as proposed by Hutchings and coworkers.[25] Notably, EtOH was present at detected level at t = 8 h. Further C_2H_6 oxidation studies were performed at elevated temperature (50 °C) with multiple initial H_2O_2 concentrations. It was found that yields of EtOOH, CH_3CHO, and CH_3COOH increased with increasing $[H_2O_2]_{initial}$ from 100 mM to 200 mM, while the yield of EtOH decreased slightly (Table S5†), indicating that increased initial quantities of H_2O_2 does not facilitate direct EtOH production. This is consistent with the results of the 21 °C reactions above (Fig. 2a), which indicated that no EtOH was observed by increasing the initial amount of H_2O_2. To further explore the origin of EtOH observed in reactions occurring at 50 °C, product solution from a representative 50 °C reaction (with quantified amounts of EtOOH and EtOH) was stored in an NMR tube, in the absence of AuPd catalysts and of H_2O_2, and the products were analyzed after 6 days and after 12 days. As shown in Fig. S5,† EtOOH was found to spontaneously decompose to EtOH in time. These 50 °C reaction studies lead to the tentative conclusion that EtOH is first derived *via* EtOOH decomposition rather than C_2H_6 oxidation, and that increased temperature promotes EtOOH decomposition to EtOH. It is also possible that EtOOH can be reduced to EtOH by H* generated by H_2O_2 decomposition.[24] These studies indicate that in these conditions a competition exists between EtOOH decomposition and EtOOH oxidation, with preference for EtOOH oxidation to CH_3CHO and CH_3COOH at relatively high H_2O_2 concentrations.

To generate a first approximation of operable reaction pathways, a series of direct oxidation studies were performed on the observed stable oxygenate products: EtOH, CH_3CHO, and CH_3COOH. An initial reactant concentration of 2 mM was selected because it is roughly the equivalent concentration of C_2H_6 in the conditions of the reactor studies above, as calculated based on known C_2H_6 solubility data. As shown in Fig. 3a, in the presence of 10 mM $[H_2O_2]_{initial}$, EtOH was oxidized primarily to CH_3CHO and CH_3COOH; CH_3CHO was primarily converted to CH_3COOH. There is evidence for C–C bond breaking in these conditions: small amounts of the C_1 oxygenates CH_3OH (MeOH) and HCOOH were observed. C_1 products have been previously observed in aqueous C_2H_6 oxidation studies, where they were proposed to originate from methyl radicals resulting from C–C scission of C_2H_6 or C_2 reaction products.[25] No liquid- or gas-phase products were observed from oxidation of CH_3COOH with a 2 mM initial concentration (higher initial concentrations are considered below). Based on these observations, a high-level reaction pathway for aqueous C_2H_6 oxidation at colloidal AuPd was generated and is shown in Fig. 3b.

This study of ethane oxidation in mild conditions is motivated by the prospect that new modes of distributed chemical manufacturing can supplement or in some cases

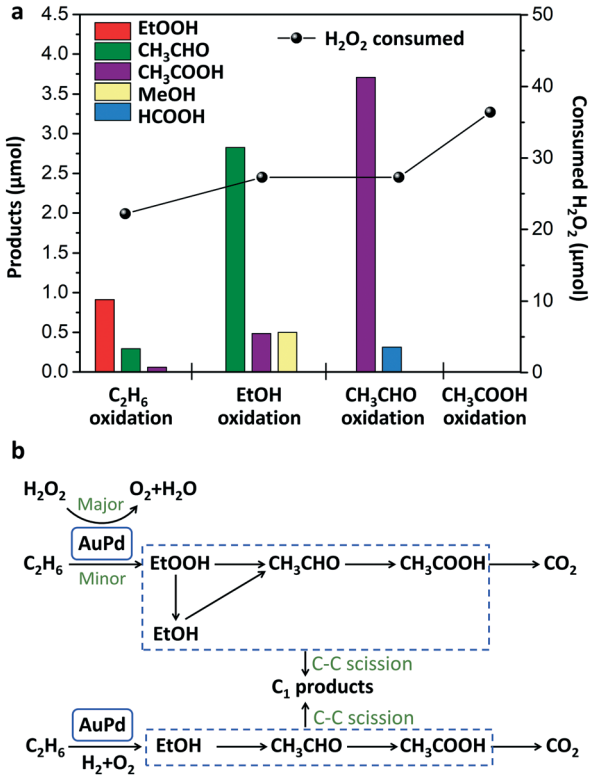

Fig. 3 (a) Quantities of products and of H_2O_2 consumed for oxidation of C_2H_6, EtOH, CH_3CHO, and CH_3COOH over AuPd. Reaction conditions: 1 mg AuPd; 21 °C; 2 h; 50 μmol H_2O_2 (10 mM $[H_2O_2]_{initial}$); 1000 rpm. For C_2H_6 oxidation 1 bar C_2H_6 was used and for oxygenate oxidation 1 bar N_2 was used, with initial 10 μmol each of EtOH, CH_3CHO, or CH_3COOH (equivalent to 2 mM initial each). (b) Schematic of pathways deduced from results of reaction studies.

displace specific production operations in the chemical industry. In this context, H_2O_2 is also a notable commodity chemical whose production is a candidate for a transition to small-scale, distributed operations. H_2O_2 can be produced safely and with minimal environmental impact through electrochemical devices[5,26] (with air and water as reactants) and thermal catalytic microreactors[27] (with air and H_2 as reactants). Additionally, the expense of H_2O_2 production through the traditional anthraquinone process[5] and its subsequent transportation is expected to place additional cost burdens on any small-scale alkane conversion facility. Although source-dependent, the cost of H_2O_2 is approximately \$0.345 per lb (50% solution), and the cost of freight is estimated to be \$3.50 per mi, regardless of the volume required for the application.[28] On-site production eliminates freight costs, and the H_2O_2 itself could be highly cost-competitive when produced in small-scale distributed facilities. For example, in a recent breakthrough in the area of distributed electrochemical H_2O_2 production, it was reported[26] that continuous streams of electrolyte-free H_2O_2 solutions, up to 20 wt%, could be produced. In that study, the cost of H_2O_2 was estimated to be \$0.07–0.15 per lb, depending on the anodic reaction employed in the system.[26]

Toward the goal of examining ethane oxidation in a distributed chemical manufacturing scenario where aqueous H_2O_2 is produced on-site at a continuous rate, additional experiments were conducted in a semi-batch configuration, wherein aqueous H_2O_2 is fed continuously during reaction. Results from the batch reactor studies shown above indicate that H_2O_2 is utilized most efficiently (highest gain factor) at low $[H_2O_2]_{initial}$. In the conditions of those experiments, 100% selectivity to EtOOH was observed at initial H_2O_2 concentrations up to 10 mM. In the continuous-feed experiments, H_2O_2 was injected into the reactor through a gas-tight syringe pump at a concentration and rate that would maintain approximately 10 mM H_2O_2 throughout the experiment (based on the calculated average consumption rate of H_2O_2 from titration experiments and by adjusting the initial solvent volume). It is stressed that the real-time concentration of H_2O_2 in the reactor cannot be measured, and that no claim is made here that the steady-state concentration is exactly 10 mM. The experiment is intended to simulate generally the relevant scenario where a valuable oxidant is fed continuously and at low concentration.

In a typical continuous-feed semi-batch reactor experiment, dilute aqueous H_2O_2 solution was injected at a constant rate into the reactor for 50 h (details of these experiments are provided in the ESI†). Through this methodology, the oxidation of C_2H_6 at 1 bar headspace pressure was examined over Au, Pd, and AuPd catalysts (Fig. 4a–c and Table S6†). Under identical reaction conditions, reactor experiments with Au and Pd yielded 3.82 and 4.63 μmol of liquid oxygenates, respectively, whereas experiments with AuPd yielded 6.51 μmol oxygenates and therefore the highest H_2O_2 gain factor. It was observed that the distribution of products differed among the reactions with the three catalysts. Product distributions from C_2H_6 oxidation over Au were weighted toward less oxidized species (*i.e.* EtOOH/EtOH) whereas those from oxidation over Pd were weighted toward more oxidized species (*i.e.* CH_3COOH). In contrast, C_2H_6 oxidation over AuPd with 50 h continuous-H_2O_2-feed yielded a product distribution centered around a species resulting from an intermediate degree of oxidation (*i.e.* CH_3CHO). These observations are consistent with expectations – it is known that Pd is associated with strong binding of O-containing intermediates and Au is associated with comparably weak interaction with these species. The binding energy of O-containing species on AuPd surfaces is closer to optimum for reaction activity. That is, the binding energy exists at a peak of the volcano curve associated with the reactivity of these species according to the Sabatier principle.[29,30] It is logical therefore that Pd catalysts were observed to favor rapid decomposition of H_2O_2 and facilitate a greater degree of product oxidation. Use of Au catalysts is not expected to favor the formation and stable adsorption of *OH and/or *OOH, preventing high rates of C_2H_6 and oxygenate activation (here, * refers to adsorbed species). The higher total yield of oxygenates over 50 h is consistent with the fact that AuPd is

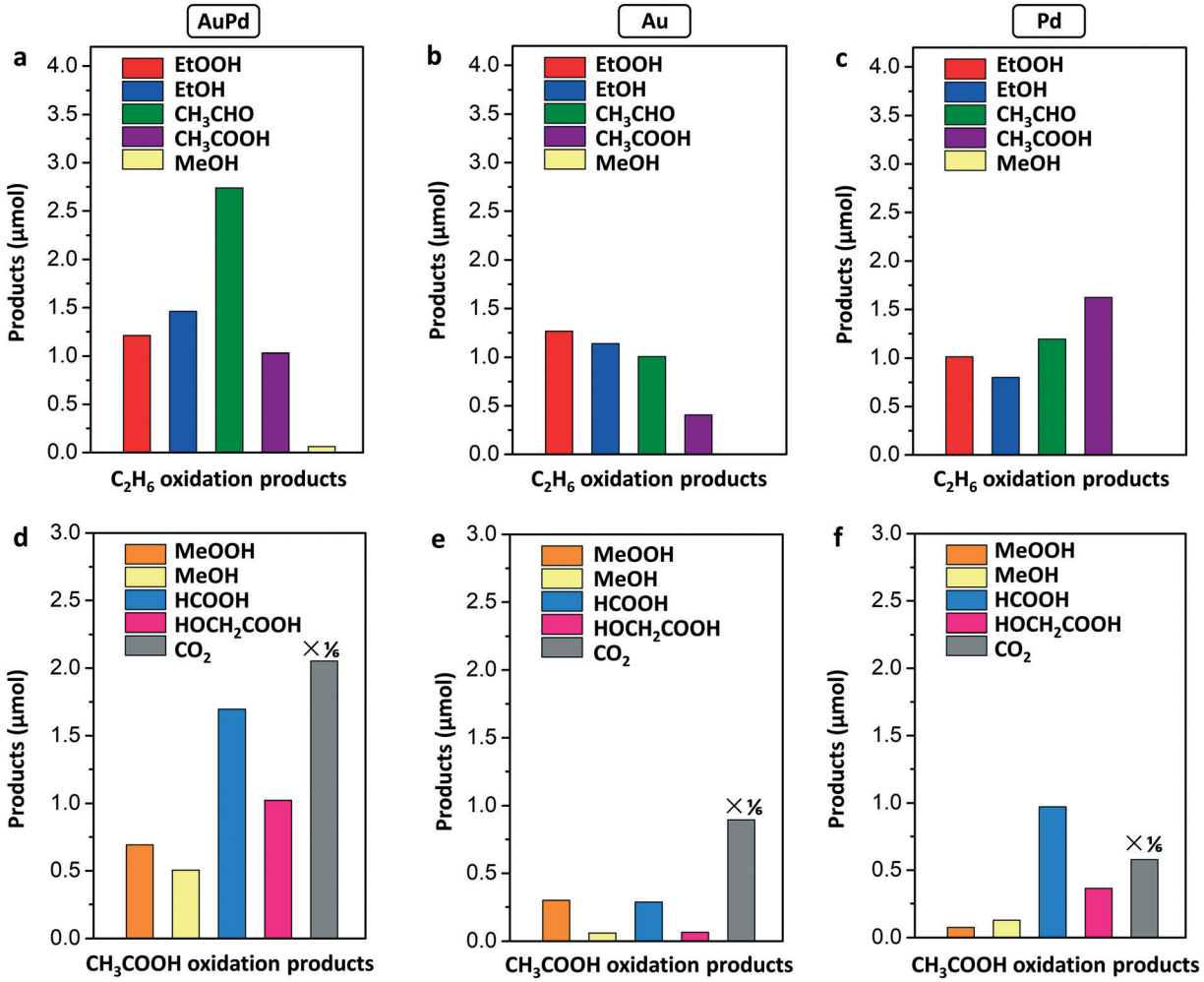

Fig. 4 (a–c) Products formed by C_2H_6 oxidation over AuPd, Au, and Pd catalysts for 50 h using the continuous-H_2O_2-feed configuration described in the main text. 1 bar C_2H_6. (d–f) CH_3COOH oxidation in the same system as (a–c). 500 μmol $[CH_3COOH]_{initial}$, 1 bar N_2. Reaction conditions: colloidal AuPd, Au, or Pd present with 6.6 μmol of metal; 21 °C; 50 h reaction time; 1000 rpm, 500 μmol H_2O_2 total injected over 50 h period.

associated with an optimal *OH and/or *OOH binding energy for this reaction.

In the conditions of the batch reactor studies above, low $[H_2O_2]_{initial}$ resulted in 100% EtOOH-selective C_2H_6 oxidation over AuPd at reaction times on the order of 1 h. However, the H_2O_2-continuous-feed semi-batch studies indicate that even at low average steady-state H_2O_2 concentration, deeper oxygenate oxidations occur (Fig. 4a). In these experiments, however, CO_2 was only observed in the headspace in extremely small quantities (Fig. S6†). This result suggested an attractive scenario could exist, wherein the most oxidized oxygenate product observed, CH_3COOH, could be stable in these catalytic conditions (room temperature and atmospheric pressure). Acetic acid, CH_3COOH, is an important compound for a number of industrial applications.[31]

Given this interest, the oxidation of aqueous CH_3COOH in the presence of Au, Pd, and AuPd was directly investigated at higher initial concentration and in the milder oxidizing conditions associated with the continuous-H_2O_2-feed configuration. Fig. 4d–f and Table S6† provide quantified product distributions associated with this reaction with 100 mM initial CH_3COOH concentration (that is, the identical experiment whose results were reported in Fig. 4a–c for C_2H_6 oxidation, but with dissolved CH_3COOH as the reactant).

In these reaction conditions and in the presence of Au, Pd, or AuPd catalysts, CO_2 was found to be a prominent CH_3-COOH oxidation product in the headspace. This indicates that when present in sufficient concentrations, CH_3COOH readily undergoes both C–H activation and C–C bond cleavage. CH_3COOH oxidation over AuPd yielded a greater overall quantity of products compared to Au and Pd, as was the case for C_2H_6 oxidation. It is clear from these results that in this reactor configuration (1 mg AuPd per 5 mL water), the combination of low temperature, low H_2O_2 concentration, and the stabilizing effect of water are insufficient to prevent overoxidation of oxygenates present in sufficiently high concentration. Specifically, at room temperature and with

100 mM initial concentration, reaction over AuPd yielded a CH_3COOH conversion of 3.25%.

The product quantities reported in Fig. 4 for C_2H_6 oxidation and CH_3COOH oxidation are not directly comparable because the concentration of the reactants differed considerably. Given the general interest in a reaction system that produces C_2 oxygenates from C_2H_6, preliminary calculations using density functional theory (DFT) were performed to determine C-H activation of C_2H_6 and CH_3COOH. Previous studies have reported that $^{\bullet}OH$ or $^{\bullet}OOH$ obtained from the decomposition of H_2O_2 are the active species for the initial activation of these molecules.[10,25,32,33] Given these precedents, barriers were calculated for H abstraction from the molecules by *OH and by *OOH on the surface of AuPd (Fig. S7 and S8†). The results, which represent a highly simplified first approximation of this reaction step, indicate H abstraction by *OH results in a lower barrier for both C_2H_6 and CH_3COOH. Recognizing that similar activation energies exist for both molecules, it is necessary to design reaction systems capable of stabilizing the oxygenates and preventing overoxidation.[13]

More generally, these results show that at low concentrations, acetic acid is relatively unreactive even in this simple aqueous system (Fig. 3a), and experiments are ongoing to determine the role of water in influencing reaction outcomes. The presence of water in similar catalytic systems – where both oxygenates and water bind to active sites through the oxygen atom – is known to effect the removal of adsorbed products, resulting in the accumulation of stable products in the solution. Encouraging results exist on this front – it has been reported that up to 0.5 M CH_3COOH produced by C_2H_6 oxidation can be stabilized in an aqueous system if H_2O_2 is produced concurrently (in tandem) at a slow and steady rate.[34]

Conclusions

This report has examined the aqueous partial oxidation of ethane over the surfaces of AuPd nanoparticle catalysts in mild conditions, with emphasis on outcomes for reactions occurring at 21 °C and 1 bar ethane (room temperature and atmospheric pressure). In these conditions, when H_2O_2 is used as an oxidant in a batch reactor, the maximum observed yield of oxygenates was 7707 μmol g_{AuPd}^{-1} h^{-1}. It was observed that ethyl hydroperoxide, ethanol, acetaldehyde, acetic acid, and small quantities of C_1 products are generated from ethane oxidation over AuPd. Supplementary experiments were performed to elucidate the most probable reaction pathways operable for C_2 oxygenate generation and subsequent oxidation in this system. It was determined that ethyl hydroperoxide is the primary product resulting from the oxidative functionalization of ethane when H_2O_2 is used as the oxidant: it is produced with 100% selectivity at short reactions times and with low initial H_2O_2 concentrations. At longer times or in more oxidizing conditions (greater H_2O_2 concentration), ethyl hydroperoxide is subsequently oxidized to acetaldehyde, which can be further oxidized to acetic acid. Ethanol is observed as a product when H_2O_2 is used as oxidant, but results indicate it originates from the decomposition of ethyl hydroperoxide rather than from the direct product of ethane oxidation. Given these observations, and motivated by the prospect of distributed manufacturing of value-added chemicals from alkane feedstocks in mild conditions, this study also reported results simulating the utilization of H_2O_2 produced on-site at continuous rates. Through use of a pressure-tight semi-batch configuration with continuous dilute H_2O_2 feed, it was determined that H_2O_2 could be utilized much more efficiently as an oxygenate-selective oxidant of ethane when low H_2O_2 concentrations are maintained for the duration of the reaction. The presented results indicate that aqueous catalytic ethane oxidation over unsupported AuPd produces a range of value-added C_2 products, but additional efforts are needed to stabilize these products from further oxidation. Given this need, a continuous process optimized for product stabilization could serve as the basis for effective distributed oxygenate synthesis in mild conditions from ethane.

Conflicts of interest

There are no conflicts to declare.

Acknowledgements

C. K. acknowledges support from American Chemical Society Petroleum Research Fund # 59999-DNI5. The authors acknowledge Prof. Ambarish Kulkarni for providing the preliminary DFT calculations. The authors acknowledge Patrick Beckett from the University of California, Davis for providing XRD measurements.

Notes and references

1 R. S. Weber, J. E. Holladay, C. Jenks, E. A. Panisko, L. J. Snowden-Swan, M. Ramirez-Corredores, B. Baynes, L. T. Angenent and D. Boysen, *WIREs Energy Environ.*, 2018, **7**, e308.
2 M. Baldea, T. F. Edgar, B. L. Stanley and A. A. Kiss, *AIChE J.*, 2017, **63**, 4262–4272.
3 J. J. Siirola, *AIChE J.*, 2014, **60**, 810–819.
4 National Academies of Sciences, Engineering, and Medicine, *The Changing Landscape of Hydrocarbon Feedstocks for Chemical Production: Implications for Catalysis: Proceedings of a Workshop*, The National Academies Press, Washington, DC, 2016, DOI: 10.17226/23555.
5 S. Yang, A. Verdaguer-Casadevall, L. Arnarson, L. Silvio, V. Čolić, R. Frydendal, J. Rossmeisl, I. Chorkendorff and I. E. L. Stephens, *ACS Catal.*, 2018, **8**, 4064–4081.
6 S. L. Foster, S. I. P. Bakovic, R. D. Duda, S. Maheshwari, R. D. Milton, S. D. Minteer, M. J. Janik, J. N. Renner and L. F. Greenlee, *Nat. Catal.*, 2018, **1**, 490–500.
7 V. L. Sushkevich, D. Palagin, M. Ranocchiari and J. A. Van Bokhoven, *Science*, 2017, **358**, eaan6083.

8 G. Prieto, *ChemSusChem*, 2017, **10**, 1056–1070.
9 R. D. Armstrong, G. J. Hutchings and S. H. Taylor, *Catalysts*, 2016, **6**, 71.
10 N. Agarwal, S. J. Freakley, R. U. Mcvicker, S. M. Althahban, N. Dimitratos, Q. He, D. J. Morgan, R. L. Jenkins, D. J. Willock, S. H. Taylor, C. J. Kiely and G. J. Hutchings, *Science*, 2017, **227**, 223–227.
11 R. D. Armstrong, S. J. Freakley, M. M. Forde, V. Peneau, R. L. Jenkins, S. H. Taylor, J. A. Moulijn, D. J. Morgan and G. J. Hutchings, *J. Catal.*, 2015, **330**, 84–92.
12 C. Hammond, R. L. Jenkins, N. Dimitratos, J. A. Lopez-Sanchez, M. H. ab Rahim, M. M. Forde, A. Thetford, D. M. Murphy, H. Hagen, E. E. Stangland, J. M. Moulijn, S. H. Taylor, D. J. Willock and G. J. Hutchings, *Chem. – Eur. J.*, 2012, **18**, 15735–15745.
13 M. Ravi, M. Ranocchiari and J. A. van Bokhoven, *Angew. Chem., Int. Ed.*, 2017, **56**, 16464–16483.
14 A. M. Venezia, V. La Parola, G. Deganello, B. Pawelec and J. L. G. Fierro, *J. Catal.*, 2003, **215**, 317–325.
15 J. S. Jirkovský, I. Panas, E. Ahlberg, M. Halasa, S. Romani and D. J. Schiffrin, *J. Am. Chem. Soc.*, 2011, **133**, 19432–19441.
16 E. Pérez-Tijerina, M. Gracia Pinilla, S. Mejía-Rosales, U. Ortiz-Méndez, A. Torres and M. José-Yacamán, *Faraday Discuss.*, 2008, **138**, 353–362.
17 C. Williams, J. H. Carter, N. F. Dummer, Y. K. Chow, D. J. Morgan, S. Yacob, P. Serna, D. J. Willock, R. J. Meyer, S. H. Taylor and G. J. Hutchings, *ACS Catal.*, 2018, **8**, 2567–2576.
18 Y. Yuan, J. Wang, S. Adimi, H. Shen, T. Thomas, R. Ma, J. P. Attfield and M. Yang, *Nat. Mater.*, 2020, **19**, 282–286.
19 S. Al-Shihri, C. J. Richard and D. Chadwick, *ChemCatChem*, 2017, **9**, 1276–1283.
20 R. McVicker, N. Agarwal, S. J. Freakley, Q. He, S. Althahban, S. H. Taylor, C. J. Kiely and G. J. Hutchings, *Catal. Today*, 2020, **342**, 32–38.
21 A. Plauck, E. E. Stangland, J. A. Dumesic and M. Mavrikakis, *Proc. Natl. Acad. Sci. U. S. A.*, 2016, **113**, E1973–E1982.
22 J. K. Edwards, S. J. Freakley, A. F. Carley, C. J. Kiely and G. J. Hutchings, *Acc. Chem. Res.*, 2014, **47**, 845–854.
23 J. K. Edwards and G. J. Hutchings, *Angew. Chem., Int. Ed.*, 2008, **47**, 9192–9198.
24 J. Kang and E. D. Park, *ChemCatChem*, 2019, **11**, 4247–4251.
25 M. M. Forde, R. D. Armstrong, C. Hammond, Q. He, R. L. Jenkins, S. A. Kondrat, N. Dimitratos, J. A. Lopez-Sanchez, S. H. Taylor, D. Willock, C. J. Kiely and G. J. Hutchings, *J. Am. Chem. Soc.*, 2013, **135**, 11087–11099.
26 C. Xia, Y. Xia, P. Zhu, L. Fan and H. Wang, *Science*, 2019, **366**, 226–231.
27 S. Maehara, M. Taneda and K. Kusakabe, *Chem. Eng. Res. Des.*, 2008, **86**, 410–415.
28 USP technologies, Solutions for clean environment, http://www.h2o2.com/faqs/FaqDetail.aspx?fId=25, accessed July 2020.
29 R. B. Rankin and J. Greeley, *ACS Catal.*, 2012, **2**, 2664–2672.
30 E. Pizzutilo, O. Kasian, C. H. Choi, S. Cherevko, G. J. Hutchings, K. J. J. Mayrhofer and S. J. Freakley, *Chem. Phys. Lett.*, 2017, **683**, 436–442.
31 P. Sherouse, *Polit. Leg. Anthropol. Rev.*, 2017, **40**, 137–157.
32 C. Hammond, M. M. Forde, M. H. Ab Rahim, A. Thetford, Q. He, R. L. Jenkins, N. Dimitratos, J. A. Lopez-Sanchez, N. F. Dummer, D. M. Murphy, A. F. Carley, S. H. Taylor, D. J. Willock, E. E. Stangland, J. Kang, H. Hagen, C. J. Kiely and G. J. Hutchings, *Angew. Chem., Int. Ed.*, 2012, **51**, 5129–5133.
33 S. Bai, F. Liu, B. Huang, F. Li, H. Lin, T. Wu, M. Sun, J. Wu, Q. Shao, Y. Xu and X. Huang, *Nat. Commun.*, 2020, **11**, 954.
34 M. Lin and A. Sen, *J. Am. Chem. Soc.*, 1992, **114**, 7307–7308.

